Toward reconstruction of the dynamics of the Universe from distant type Ia supernovae

Marek Szydłowski* and Wojciech Czaja†
Astronomical Observatory, Jagielonian University, Orla 171, 30-244, Kraków, Poland
(Received 6 September 2003; published 9 April 2004)

We describe a model-independent method of estimating the qualitative dynamics of an accelerating universe from observations of distant type Ia supernovae. Our method is based on the luminosity-distance function, optimized to fit observed distances of supernovae, and the Hamiltonian representation of dynamics for the quintessential universe with a general form of the equation of state $p=w[a(z)]\rho$. Because of the Hamiltonian structure of Friedmann-Robertson-Walker (FRW) dynamics with the equation of state $p=w[a(z)]\rho$, the dynamics is uniquely determined by the potential function $V(a)$ of the system. The effectiveness of this method in the discrimination of model parameters of the Cardassian evolution scenario is also given. Our main result is the following: restricting consideration to the flat model with the current value of $\Omega_{m,0}=0.3$, the constraints at a 2σ confidence level to the presence of ρ^n modification of the FRW models are $-0.50\lesssim n\lesssim 0.36$.

DOI: 10.1103/PhysRevD.69.083507 PACS number(s): 98.80.Bp, 11.25.−w, 98.80.Cq

I. INTRODUCTION

Recent observations of type Ia supernovae (SNIa) [1–3] supported by Wilkinson Microwave Anisotropy Probe (WMAP) measurements of the anisotropy of the angular temperature fluctuations [4] indicate that our Universe is spatially flat and accelerating. On the other hand, the power spectrum of galaxy clustering [5] indicates that about 30% of the critical density of the Universe should be in the form of nonrelativistic matter (cold dark matter and baryons). The remaining, almost two-thirds of the critical energy, may be in the form of a component having negative pressure (dark energy). Although the nature of dark energy is unknown, the positive cosmological constant term seems to be a serious candidate for the description of dark energy. In this case the cosmological constant Λ and energy density $\varepsilon_\Lambda=\Lambda/(8\pi G)$ remain constant with time and the corresponding mass density $\rho_\Lambda\equiv\varepsilon_\Lambda/c^2=6.44\times10^{-30}(\Omega_\Lambda/0.7)\times(h/0.7)\ \mathrm{g\,cm^{-3}}$, where h is the Hubble constant H_0 expressed in units of $100\ \mathrm{km\,s^{-1}\,Mpc^{-1}}$ and $\Omega_\Lambda=0.7\pm0.1$. Although the cold dark matter (CDM) model with a cosmological constant and dust provides an excellent explanation of the SNIa data, the present value of Λ is $\sim10^{123}$ times smaller than the value predicted by the particle physics model. Many alternative candidates for dark energy have been advanced and some of them are in good agreement with the current observational constraints [6–12]. Moreover, it is a natural suggestion that the Λ term has a dynamical nature as in the inflationary scenario. Therefore, it is reasonable to consider the next simplest form of a dark energy alternative to the cosmological constant ($w=-1$) for which the equation of state depends upon time in such a way that $p=w[a(z)]\rho$, where $w\equiv p/\rho$ is a coefficient of the equation of state parametrized by the scale factor or redshift. It has been demonstrated [13,14] that the dynamics of such a system can be represented by the one-dimensional Hamiltonian flow

$$\mathcal{H}=\frac{\dot{a}^2}{2}+V(a), \tag{1}$$

where the overdot means differentiation with respect to the cosmological time t and $V(a)$ is a potential function of the scale factor a given by

$$V(a)=-\frac{\rho_{\mathrm{eff}}(a)}{6}a^2, \tag{2}$$

where ρ_{eff} is the effective energy density, which satisfies the conservation condition

$$\dot{\rho}_{\mathrm{eff}}=-3\frac{\dot{a}}{a}(\rho_{\mathrm{eff}}+p_{\mathrm{eff}}).$$

For example, for the CDM model with a cosmological constant (ΛCDM) model we have

$$\rho_{\mathrm{eff}}=\Lambda+\rho_{m,0}a^{-3},$$

$$p_{\mathrm{eff}}=-\Lambda+0. \tag{3}$$

Of course the trajectories of the system lie on the zero energy surface $\mathcal{H}\equiv0$.

The Hamiltonian (1) can be rewritten in the following form convenient for our current reconstruction of the equation of state from the potential function V:

$$\mathcal{H}(p_x,x)=\frac{p_x^2}{2}+V(x), \tag{4}$$

where $p_x=\partial L/\partial\dot{x}$. Here overdot means differentiation with respect to some new reparametrized time $t\to\tau: d\tau=|H_0|dt$, $x\equiv a/a_0=(1+z)^{-1}$.

For example, for a mixture of noninteracting fluids the potential $V(x)$ takes the form

$$V(x)=-\frac{1}{2}\sum_i \Omega_{i,0}x^{2-3(w_i+1)}, \tag{5}$$

*Electronic address: uoszydlo@cyf-kr.edu.pl
†Electronic address: czaja@oa.uj.edu.pl

where $p_i = w_i \rho_i$ for the ith fluid and $\forall\ i w_i = \text{const}$ (similar to the quiessence model of dark energy).

Due to the Hamiltonian structure of Friedmann-Robertson-Walker (FRW) dynamics, with the general form of the equation of state $p = w[a(z)]\rho$, the dynamics is uniquely determined by the potential function $V(a)$ [or $V(x)$] of the system. Only for simplicity of presentation we assume that the universe is spatially flat (in the opposite case the trajectories of the system should be considered at the energy level $\mathcal{H} = \frac{1}{2}\Omega_{k,0}$).

Let us note that from the potential function we can obtain the equation of state coefficient $w = p/\rho$,

$$w = -\frac{1}{3}\left(1 + \frac{d(\ln V)}{d(\ln a)}\right). \tag{6}$$

The term $d(\ln V)/d(\ln a)$ has a simple interpretation as an elasticity coefficient of the potential function with respect to the scale factor.

Thus from the potential function V both $\rho(a)$ and p can be unambiguously calculated:

$$\rho(a) = -6\frac{V(a)}{a^2},$$

$$p = 2\frac{V(a)}{a^2}\left(1 + \frac{d(\ln V)}{d(\ln a)}\right). \tag{7}$$

II. THE EXPANSION SCENARIO FROM SUPERNOVAE DISTANCES

As is well known, in a flat FRW cosmology the luminosity distance d_L and the coordinate distance r to an object at redshift z are simply related as

$$a_0 r = a_0 \int_t^{t_0} \frac{dt'}{a(t')} = \frac{d_L(z)}{1+z} \tag{8}$$

($c = 8\pi G = 1$ here and elsewhere). From Eq. (8) the Hubble parameter is given by

$$H(z) = [\ln \dot{a}] = \left[\frac{d}{dz}\left(\frac{d_L(z)}{1+z}\right)\right]. \tag{9}$$

It is crucial that the formula (9) is purely kinematic and depends on neither the microscopic model of matter, including the Λ term, nor the dynamical theory of gravity. Due to the existence of such a relation it is possible to calculate the potential function, which is

$$V(a) = -\frac{1}{2}H^2 a^2 = -\frac{\{(d/dz)[d_L(z)/(1+z)]\}^{-2}}{2(1+z)^2}. \tag{10}$$

This in turn allows us to reconstruct the potential $V(z)$ from SNIa data. Let us note that $V(z)$ depends on the first derivative with respect to z whereas $w(z)$ is associated with the second derivative.

Let us also note that the one-dimensional potential function for a particle-universe moving in the configurational a (or x) space can be reconstructed from recent measurements of the angular size of high-z compact radio sources compiled by Gurvits *et al.* [15]. The corresponding formula is

$$V(a) = -\frac{\{(d/dz)[d_A(z)(1+z)]\}^{-2}}{2(1+z)^2}, \tag{11}$$

where the luminosity distance d_L and the angular distance d_A are related by the simple formula

$$d_L(z) = (1+z)^2 d_A(z). \tag{12}$$

Since the potential function is related to the luminosity function by relation (10) one can determine both the class of trajectories in the phase plane $(a, \dot{a})$ and the Hamiltonian form as well as reconstructing the quintessence parameter $w(z)$ provided that the luminosity function $d_L(z)$ is known from observations.

Now we can reconstruct the form of the potential function (10) using a natural ansatz introduced by Sahni *et al.* [16]. In this approach the dark energy density that coincides with ρ_{eff} is given as a truncated Taylor series with respect to $u = (1+z)$:

$$\rho_{\text{DE}} = \rho_{\text{eff}} = A_0 + A_1 u + A_2 u^2.$$

This leads to

$$H(z) = H_0\sqrt{\Omega_{m,0}(1+z)^3 + A_0 + A_1(1+z) + A_2(1+z)^2} \tag{13}$$

and

$$\frac{d_L(z)}{(1+z)} = \frac{1}{H_0} \times \int_0^z \frac{dz}{\sqrt{\Omega_{m,0}(1+z)^3 + A_0 + A_1(1+z) + A_2(1+z)^2}}. \tag{14}$$

The values of the three parameters A_0, A_1, A_2 can be obtained by applying a standard fitting procedure to SNIa observational data based on the maximum likelihood method.

The potential function (10) written in terms of $(1+z)$ is

$$V[a(z)] = -\frac{\rho_{\text{eff}} a^2}{6} = -\frac{1}{2}H_0^2[\Omega_{m,0}(1+z) + A_0(1+z)^{-2} + A_1(1+z)^{-1} + A_2] \tag{15}$$

or in dimensionless form

$$V[x(z)] = -\frac{1}{2}[\Omega_{m,0}x^{-1} + \Omega_{\Lambda,0}x^2 + \Omega_{t,0}x + \Omega_{k,0}], \tag{16}$$

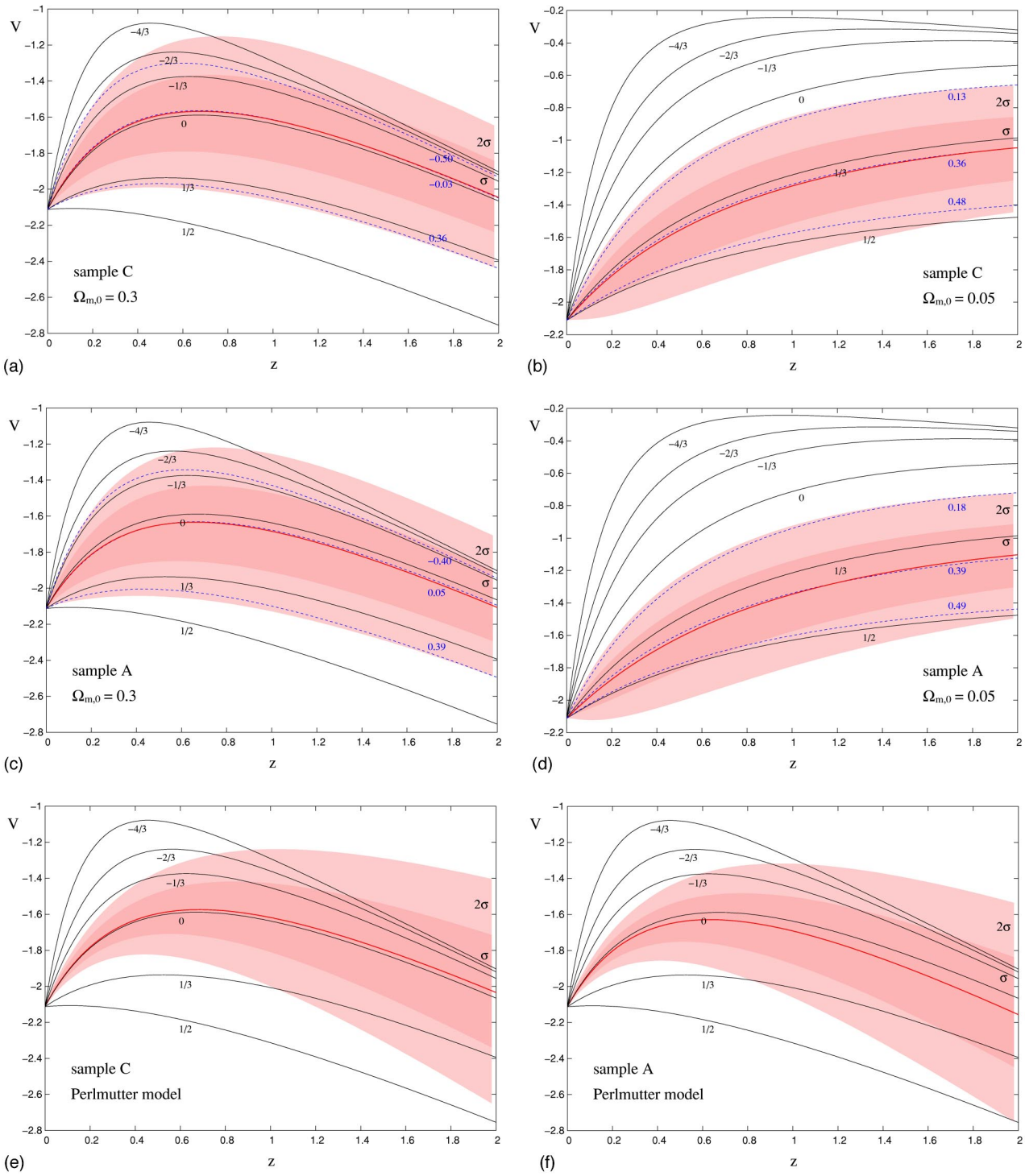

FIG. 1. (Color online) Confidence levels for the potential function V for the model with (a) $A_3=0.3$ (sample C), (b) $A_3=0.05$ (sample C), (c) $A_3=0.3$ (sample A), (d) $A_3=0.05$ (sample A), and for the Perlmutter model (e) (sample C) and (f) (sample A). The best fit for each model is represented by the bold line. Solid and dashed lines represent potential functions for theoretical Cardassian models for $\Omega_{m,0}=0.3$ [(a),(b),(e),(f)] and 0.05 [(c),(d)] and $n=1/2,1/3,0,-1/3,-2/3,-4/3$.

where $A_i/(3H_0^2)=\Omega_{i,0}(i=\Lambda,t,k)$.

Our approach to the reconstruction of the dynamics of the model is different from the standard approach in which $w(z)$ is determined directly from the luminosity-distance formula. It should be stressed that the latter approach has an inevitable limitation because the luminosity-distance dependence on $w(z)$ is obtained through a multiple-integral relation that loses detailed information on $w(z)$ [17]. In our approach the reconstruction is simpler (only a single integral is required). Our approach is also different from the concept of recon-

TABLE I. Fitting results of the statistical analysis from distant type Ia supernovae data. The best fit and most probable values of parameters A_i and $\mathcal{M}$ for the polynomial fit (14) for sample A of Perlmutter SNIa data.

	A_0	A_1	A_2	A_3	$\mathcal{M}$	χ^2	$z_{\max}$	$V_{\max}$
Best fit	0.61	0.09	0.00	0.30	-3.38	96.03	0.659	-1633.21
Max(P)	$0.60^{+0.40}_{-0.43}$	$0.09^{+0.43}_{-0.40}$	0.00	0.30	$-3.38^{+0.06}_{-0.06}$			
Best fit	-0.25	1.20	0.00	0.05	-3.37	96.84	3.677	-1011.88
Max(P)	$-0.26^{+0.38}_{-0.44}$	$1.20^{+0.44}_{-0.38}$	0.00	0.05	$-3.36^{+0.06}_{-0.06}$			

struction of the potential of scalar fields considered in the context of quintessence [8].

The key steps of our method are the following.

(1) We reconstruct the potential function $V(a)$ for the Hamiltonian dynamics of the quintessential universe from the luminosity distances of supernovae type Ia;

(2) we draw the best fit curves and confidence level regions obtained from the statistical analysis of SNIa data;

(3) we set the theoretically predicted forms of the potential functions on the confidence level diagram;

(4) those theoretical potentials that are even partially outside the 2σ confidence level are treated as being unfitted to observations; and

(5) we choose the potential function that lies near the best fit curve.

Our reconstruction is an effective statistical technique which can be used to compare a large number of theoretical models with observations. Instead of estimating some relevant parameters for each model separately, we choose a model-independent fitting function and perform a maximum likelihood parameter estimation for it. The confidence levels obtained can be used to discriminate between the models considered. In this paper this technique is used to find the fitting function for the luminosity distance.

The additional argument which is important when considering the potential $V(a)$ is that it allows us to find some modification in the Friedmann equations as in the ''Cardassian expansion scenario'' [18]. This proposition is very intriguing because of additional terms, which automatically cause the acceleration of the universe [19–22]. These modifications come from the fundamental physics and these terms can be tested using astronomical observations of distant type Ia supernovae. With this aim the recent measurements of the angular size of high-redshift compact radio sources can also be used [15].

The important question is the reliability of the data available. We expect that supernovae data will improve greatly over the next few years. The SNAP mission should give us about 2000 type Ia supernovae cases each year. This satellite mission and the next planned ones will increase the accuracy of the data compared to data from the 1990s. In our analysis we use the available data starting from the three Perlmutter samples (sample A is the complete sample of 60 supernovae, but in the analysis we also used samples B and C, in which four and six outliers, respectively, were excluded). The fit for the sample C is more robust and this sample was accepted as the basis of our consideration. For technical details of the method the reader is referred to our previous two papers [13,14].

In Fig. 1 we show the reconstructed potential function obtained using the fitting values of A_i as well as $\mathcal{M}$. The bold line represents the potential function for the best fit values of the parameters (see Tables I, II and III). In each case the shaded areas cover the confidence levels 68.2% (1σ) and 95.4% (2σ) for the potential function. The different forms of the potential function that are obtained from the theory are presented in the confidence levels. Here we consider one case, namely, the Cardassian model. In this case the standard FRW equation is modified by the presence of an additional ρ^n term, where ρ is the energy density of matter and radiation. For simplicity we assume that the density parameter for radiation is zero (see Table IV). The Cardassian scenario is proposed as an alternative to the cosmological constant in explaining the acceleration of the Universe. In this scenario the Universe automatically accelerates without any dark energy component. The additional term in the Friedmann equation arises from exotic physics of the early universe (i.e., in the brane cosmology with Randall-Sundrum version $n=2$).

Let us note that there is a simple interpretation of the Cardassian term as an additional noninteracting fluid with pressure $p=[n(1+w)-1]\rho$, where the standard term is obtained from the fluid $p=w\rho$ and $w=$const. In the special

TABLE II. Fitting results of the statistical analysis from distant type Ia supernovae data. The best fit values of parameters A_i and $\mathcal{M}$ for the polynomial fit (14) for sample C of Perlmutter SNIa data. The fit is more robust, because the two very likely reddened supernovae SN1996cg and SN1996cn have been removed [3].

	A_0	A_1	A_2	A_3	$\mathcal{M}$	χ^2	$z_{\max}$	$V_{\max}$
Best fit	0.74	-0.04	0.00	0.30	-3.43	53.28	0.676	-1567.33
Max(P)	$0.73^{+0.40}_{-0.44}$	$0.04^{+0.44}_{-0.40}$	0.00	0.30	$-3.43^{+0.06}_{-0.06}$			
Best fit	-0.13	1.08	0.00	0.05	-3.42	53.83	3.522	-968.74
Max(P)	$-0.14^{+0.40}_{-0.44}$	$1.08^{+0.44}_{-0.39}$	0.00	0.05	$-3.41^{+0.06}_{-0.06}$			

TABLE III. Fitting results of the statistical analysis for the Perlmutter model and both (A and C) samples of Perlmutter SNIa data.

	Sample	$\Omega_{\Lambda,0}$	$\Omega_{m,0}$	$\mathcal{M}$	χ^2	$z_{\max}$	$V_{\max}$
Best fit	C	0.71	0.29	-3.43	53.29	0.684	-1573.69
Max(P)	C	$0.70^{+0.05}_{-0.05}$	$0.30^{+0.05}_{-0.05}$	-3.43			
Best fit	A	0.69	0.31	-3.39	96.00	0.632	-1628.31
Max(P)	A	$0.68^{+0.05}_{-0.05}$	$0.32^{+0.05}_{-0.05}$	-3.39			

case of dust we obtain $p=(n-1)\rho$. The effective energy density can be modeled by some kind of quintessence matter with the equation of state

$$p_{\text{eff}}=w(a)\rho_{\text{eff}},$$

where

$$w(a) = \frac{(n-1)\Omega_{\text{C},0}}{\Omega_{\text{m},0}a^{3(n-1)}+\Omega_{\text{C},0}}. \tag{17}$$

The solid lines in Fig. 1 represent the potential functions for the different Cardassian scenarios of an accelerated expansion of the universe.

For visualizing the quality of the fitting procedure performed the Hubble diagrams are presented on Fig. 2.

The general conclusion from our statistical analysis is that the potential function has a maximum at some $z=z_0$ (or $a=a_0$) and that

$$\frac{\partial^2 V}{\partial a^2}(z)<0. \tag{18}$$

In the next section it will be demonstrated that the reconstructed potential function contains all the information that we need for reconstruction of the dynamics of any cosmological model on the phase plane.

III. APPLICATION: TOWARD THE RECONSTRUCTION OF PHASE PORTRAIT AND MODEL PARAMETERS

The dynamics of the considered cosmological models is governed by the dynamical system

$$\dot{x}\equiv\frac{dx}{dt}=y,$$

$$\dot{y}\equiv\frac{dy}{dt}=-\frac{\partial V}{\partial x}, \tag{19}$$

with the first integral for Eq. (19) $\mathcal{H}=0\Leftrightarrow\dot{x}^2/2+V(x)=0$. The main aim of dynamical system theory is the investigation of the space of all solutions (19) for all possible initial conditions, i.e., phase space $\mathbb{M}$. In the context of quintessential models with the equation of state $p=w[a(z)]\rho$ there exists a systematic method of reducing Einstein's field equations to the form of the dynamical system (19) [13]. One of the features of such a representation of the dynamics is the possibility of resolving some cosmological problems like the horizon and flatness problems in terms of the potential function $V(x)$.

The phase space $\mathbb{M}$ (or state space) is a natural visualization of the dynamics of any model. Every point $P=(x,y)\in\mathbb{M}$ corresponds to a possible state of the system. The right-hand sides of the system (19) define a vector field $\mathbf{F}(P)=[y,-\partial V/\partial x]$ belonging to the tangent space $T_p\mathbb{M}$. Integral curves of this vector field define a one-parameter group of diffeomorphisms $\phi(P)$ called the phase flow. In the phase space the phase curves [orbits of the group $\phi(P)$] represent the evolution of the system whereas the critical points y

TABLE IV. The potential functions in dimensionless form for two cases: the ΛCDM model and Cardassian scenario.

	Form of the potential function	Position of the maximum predicted by theoretical models	Position of the maximum from reconstruction	
			Sample	Value
Perlmutter model	$V(x)=-\frac{1}{2}[\Omega_{m,0}x^{-1}+\Omega_{\Lambda,0}x^2]$	$x_0=\sqrt[3]{\frac{1}{2}\frac{\Omega_{m,0}}{1-\Omega_{m,0}}}$	A	0.613
			C	0.594
Cardassian scenario	$V(x)=-\frac{1}{2}[\Omega_{m,0}x^{-1}+\Omega_{C,0}x^{2-3n}]$	$x_0=\left[(2-3n)\left(\frac{1}{\Omega_{m,0}}-1\right)\right]^{1/3(n-1)}$	A	0.598
			C	0.599

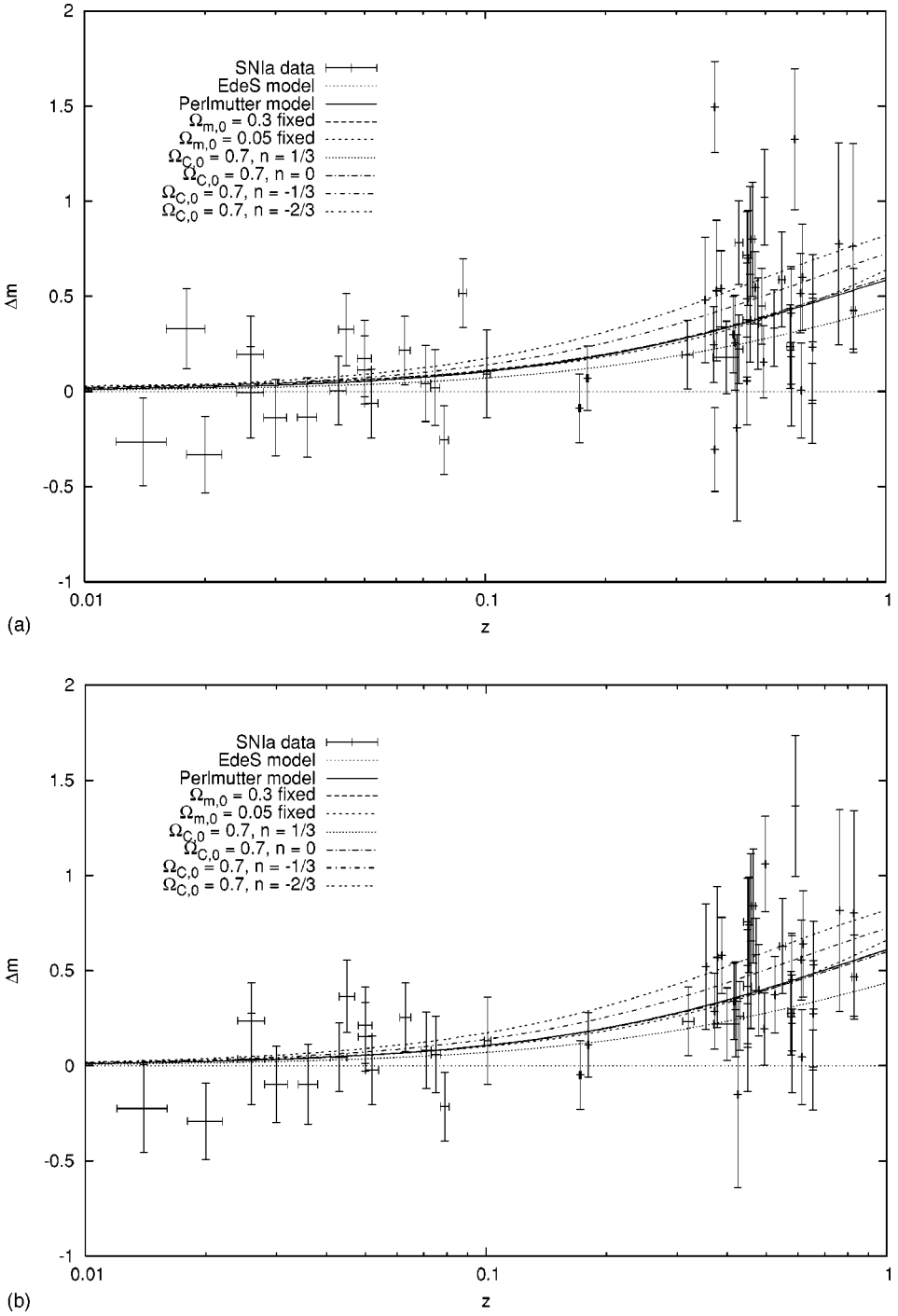

FIG. 2. Hubble diagrams for Perlmutter SNIa data for samples A (a) and C (b). The different type lines represent the best fitted magnitude-redshift relations (the Perlmutter model and polynomial fits with fixed $\Omega_{m,0}$ parameters) and hypothetical Cardassian scenarios for different values of the parameters $\Omega_{C,0}$ and n.

$=0$, $\partial V/\partial x=0$ are singular solutions—equilibria from the physical point of view. The phase curves together with the critical points constitute the phase portrait of the system (see Figs. 3 and 4).

Now we can define the equivalence relation between two phase portraits (or two vector fields) by the topological equivalence, namely, two phase portraits are equivalent if there exists an orientation-preserving homeomorphism transforming integral curves of both systems into each other. Following the Hartman-Grobman theorem, the behavior of the system near hyperbolic critical points ($\forall\ i\ \mathrm{Re}\,\lambda_i\neq 0$, where λ_i is the appropriate eigenvalue of the linearization matrix $\mathcal{A}$ of the dynamical system) is equivalent to the behavior of its linear part

$$\dot{x}=y,\quad \dot{y}=-\left(\frac{\partial^2 V}{\partial x^2}\right)_{(x=x_0,0)}(x-x_0). \tag{20}$$

In our case the linearization matrix takes the form

$$\mathcal{A}=\begin{bmatrix} 0, & 1 \\ -\partial^2 V/\partial x^2, & 0 \end{bmatrix}_{(x_0,0)}. \tag{21}$$

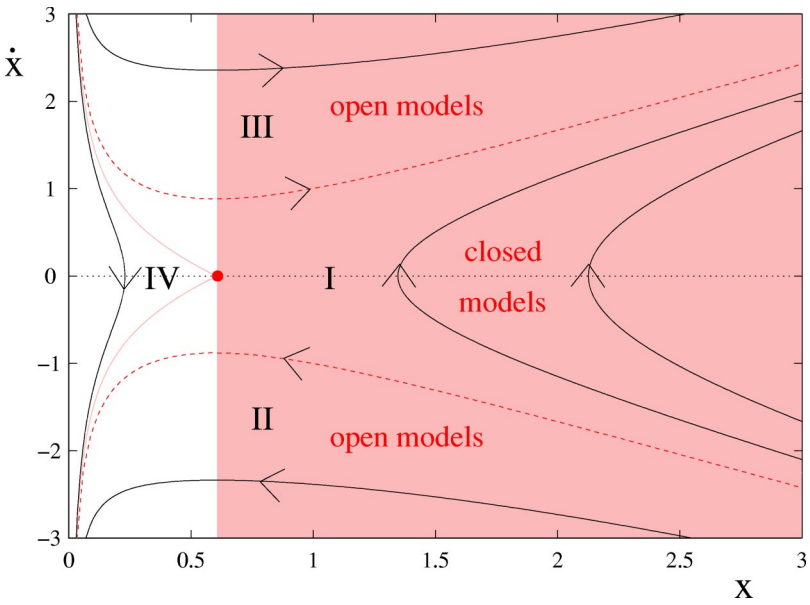

FIG. 3. (Color online) Phase space for the system (19) reconstructed from the potential function (16) for the best fitted parameters (Table I, $A_3=0.3$). The shaded domain of phase space is the domain of accelerated expansion of the Universe. The dashed line represents the flat model trajectory which separates regions with negative and positive curvatures.

Classification of the critical points is given in terms of the eigenvalues of the linearization matrix since the eigenvalues can be determined from the characteristic equation $\lambda^2-(\mathrm{Tr}\,\mathcal{A})\lambda+\det\mathcal{A}=0$. In our case $\mathrm{Tr}\,\mathcal{A}=0$ and the eigenvalues are either real if $(\partial^2V/\partial x^2)|_{(x_0,0)}<0$ or purely imaginary and mutually conjugated if $(\partial^2V/\partial x^2)|_{(x_0,0)}>0$. In the former case the critical points are saddles and in the latter case they are centers.

The advantage of representing the dynamics in terms of the Hamiltonian (1) is the possibility of discussing the stability of the critical points, which is based only on the convexity of the potential function. In our case the only possible critical points in a finite domain of phase space are centers or saddles.

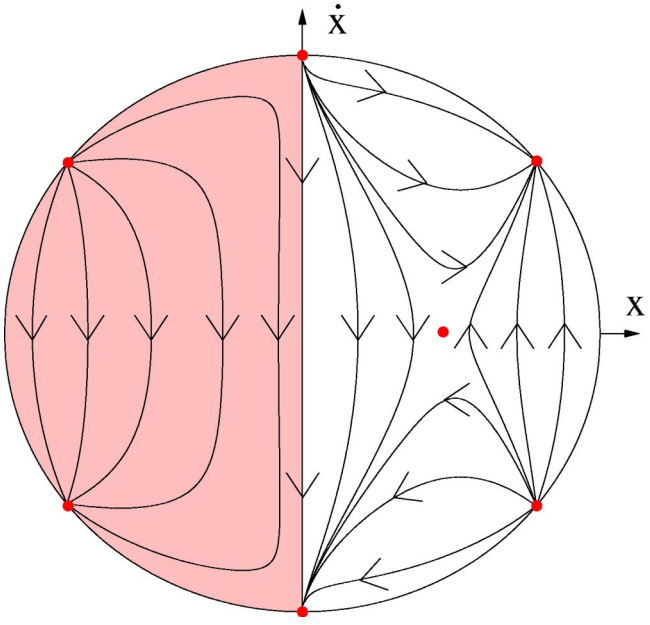

FIG. 4. (Color online) Phase space shown in Fig. 3 transformed on the compact Poincaré sphere. Nonphysical domain of phase space is shaded.

The dynamical system is said to be structurally stable if all other dynamical systems (close to it in a metric sense) are equivalent to it. Two-dimensional dynamical systems on compact manifolds form an open and dense subset in the space of all dynamical systems on the plane [23]. Structurally stable critical points on the plane are saddles, nodes, and limit cycles whereas centers are structurally unstable. There is a widespread opinion among scientists that each physically realistic model of the Universe should possess some kind of structural stability—because the existence of many drastically different mathematical models, all in agreement with observations, would be fatal for the empirical method of science [24].

Based on the reconstructed potential function one can conclude the following.

(1) Since the diagram of the potential function $V[a(z)]$ is convex up and has a maximum which corresponds to a single critical point, the quantity $(\partial^2V/\partial a^2)|_{(a_0,0)}<0$ at the critical point (saddle point) and the eigenvalues of the linearization matrix at this point are real with opposite signs.

(2) The model is structurally stable, i.e., small perturbations of it do not change the structure of the trajectories in the phase plane.

(3) Since $\ddot{a}=-\partial V/\partial a$ one can easily conclude from the geometry of the potential function that in the accelerating region $(\ddot{a}>0)$ $V(a)$ is a decreasing function of its argument.

(4) The reconstructed phase portrait for the system is equivalent to the portrait of a model with matter and a cosmological constant.

By an inspection of the phase portraits we can distinguish four characteristic regions in the phase space. The boundaries of region I are formed by a separatrix coming out from the saddle point and going to the singularity and another separatrix coming out of the singularity and approaching the saddle. This region is covered by trajectories of closed and recollapsing models with initial and final singularities.

The trajectories moving in region IV are also confined by a separatrix and they correspond to closed universes contracting from the unstable de Sitter node toward the stable de Sitter node.

The trajectories situated in region III correspond to models expanding toward a stable de Sitter node at infinity. Similarly, the trajectories in the symmetric region II represent universes contracting from the unstable node toward the singularity.

The main idea of the qualitative theory of differential equations is the following. Instead of finding and analyzing an individual solution of the model one investigates the space of all possible solutions. Any property (for example acceleration) is believed to be realistic if it can be attributed to a large subsets of models within the space of all solutions or if it possesses some stability property that is shared by all slightly perturbed models.

IV. CONCLUSION

The possible existence of the unknown form of matter called dark energy has usually been invoked as the simplest way to explain the recent observational data of SNIa. However, the effects arising from new fundamental physics can also mimic the gravitational effects of dark energy through a modification of the Friedmann equation.

We exploited the advantages of our method to discriminate among different dark energy models. With the independently determined density parameter of the Universe ($\Omega_{m,0}=0.3$) we found that the current observational results require the cosmological constant $n\simeq 0$ in Cardassian models. On Fig. 1 we can see that in both cases of sample A (Fig. 1c) and sample C (Fig. 1a) n should be close to zero. Similarly, if we assume that the density parameter for baryonic matter is $\Omega_{m,0}=0.05$ then $n\simeq 0.36$ in the case of sample C (Fig. 1b) and $n\simeq 0.39$ for sample A (Fig. 1d). Moreover, we showed (for sample C of the Perlmutter SNIa data) that a simple Cardassian model as a candidate for dark energy is ruled out by our analysis at the confidence level 2σ if $n\gtrsim 0.36$ and $n\lesssim -0.50$ for $\Omega_{m,0}=0.3$ and if $n\gtrsim 0.48$ and $n\lesssim 0.13$ for $\Omega_{m,0}=0.05$.

Our main result is that the structure of the phase space of accelerating models can be reconstructed from SNIa data. It is a consequence of the fact that the potential of the Hamiltonian system describing the dynamics of accelerating models can be obtained from the d_L relation for distant supernovae of type Ia. We demonstrate that all information about the structure of the phase space is contained in the potential function, which gives the Hamiltonian flow.

ACKNOWLEDGMENTS

The authors are very grateful to Dr. A. Krawiec and Dr. W. Godłowski for discussions and comments. This work was supported by KBN grant No. 1 P03D 003 26.

[1] A.G. Riess *et al.*, Astron. J. **116**, 1009 (1998).
[2] A.G. Riess *et al.*, Astrophys. J. **560**, 49 (2002).
[3] S.J. Perlmutter *et al.*, Astrophys. J. **517**, 565 (1999).
[4] A. Benoit *et al.*, Astron. Astrophys. **399**, 25 (2003).
[5] W.J. Parcival *et al.*, Mon. Not. R. Astron. Soc. **337**, 1068 (2002).
[6] B. Ratra and P.J.E. Peebles, Phys. Rev. D **37**, 3406 (1998).
[7] P.J.E. Peebles and B. Ratra, Rev. Mod. Phys. **75**, 559 (2003).
[8] R.R. Caldwell, R. Dave, and P.J. Steinhardt, Phys. Rev. Lett. **80**, 1582 (1998).
[9] A. Kamenshchik, U. Moschella, and V. Pasquier, Phys. Lett. B **511**, 265 (2001).
[10] C. Armendariz-Picon, V. Mukhanov, and P.J. Steinhardt, Phys. Rev. Lett. **85**, 4438 (2000).
[11] M. Bucher and D. Spergel, Phys. Rev. D **60**, 043505 (1999).
[12] L. Parker and A. Raval, Phys. Rev. D **60**, 063512 (1999).
[13] M. Szydlowski and W. Czaja, Phys. Rev. D (to be published), gr-qc/0305033.
[14] M. Szydlowski and W. Czaja, Phys. Rev. D **69**, 023506 (2004).
[15] L.I. Gurvits, K.I. Kellermann, and S. Frey, Astron. Astrophys. **342**, 378 (1999).
[16] V. Sahni and A. Starobinsky, Int. J. Mod. Phys. D **9**, 373 (2000).
[17] I. Maor, R. Brustein, and P.J. Steinhardt, Phys. Rev. Lett. **86**, 6 (2001).
[18] K. Freese and M. Lewis, Phys. Lett. B **540**, 1 (2002).
[19] J.S. Alcaniz and J.A.S. Lima, Astrophys. J. Lett. **521**, L87 (1999).
[20] P.P. Avelino, L.M.G. Beca, J.P.M. de Carvalho, C.J.A.P. Martins, and P. Pinto, Phys. Rev. D **67**, 023511 (2003).
[21] Z. Zhu and M. Fujimoto, Astrophys. J. **581**, 1 (2002).
[22] Z. Zhu and M. Fujimoto, Astrophys. J. **585**, 52 (2003).
[23] M. Peixoto, Topology **1**, 101 (1962).
[24] R. Thom, *Stabilité Structurelle et Morphogénèse* (Inter Editions, Paris, 1977).